the FEBS Journal

A pre-docking role for microtubules in insulin-stimulated glucose transporter 4 translocation

Yu Chen*, Yan Wang*, Wei Ji*, Pingyong Xu and Tao Xu

National Key Laboratory of Biomacromolecules, Institute of Biophysics, Chinese Academy of Sciences, Beijing, China

Keywords
GLUT4; intracellular transport; microtubules; TIRFM; vesicle docking

Correspondence
T. Xu or P. Xu, Institute of Biophysics, Chinese Academy of Sciences, Beijing 100101, China
Fax: +86 10 64867566
Tel: +86 10 64888469
E-mail: xutao@ibp.ac.cn or pyxu@moon.ibp.ac.cn

*These authors contributed equally to this work

(Received 6 November 2007, revised 6 December 2007, accepted 11 December 2007)

doi:10.1111/j.1742-4658.2007.06232.x

Insulin stimulates glucose uptake by inducing translocation of glucose transporter 4 (GLUT4) from intracellular resides to the plasma membrane. How GLUT4 storage vesicles are translocated from the cellular interior to the plasma membrane remains to be elucidated. In the present study, intracellular transport of GLUT4 storage vesicles and the kinetics of their docking at the plasma membrane were comprehensively investigated at single vesicle level in control and microtubule-disrupted 3T3-L1 adipocytes by time-lapse total internal reflection fluorescence microscopy. It is demonstrated that microtubule disruption substantially inhibited insulin-stimulated GLUT4 translocation. Detailed analysis reveals that microtubule disruption blocked the recruitment of GLUT4 storage vesicles to underneath the plasma membrane and abolished the docking of them at the plasma membrane. These data suggest that transport of GLUT4 storage vesicles to the plasma membrane takes place along microtubules and that this transport is obligatory for insulin-stimulated GLUT4 translocation.

Blood glucose concentration is tightly and acutely regulated in mammals. The major mechanism that diminishes blood glucose when carbohydrates are ingested is insulin-stimulated increase of glucose uptake by skeletal muscle and adipocytes [1]. The principle glucose transporter protein mediating this insulin-stimulated glucose uptake is glucose transporter 4 (GLUT4) [2,3]. In unstimulated cells, rapid endocytosis, slow exocytosis and dynamic or static retention cause GLUT4 to concentrate in intracellular pools [4,5]. Insulin stimulation results in GLUT4 translocation from its intracellular locations to the plasma membrane (PM) and gain of GLUT4 on the cell surface increases glucose uptake [2,6]. Sequential activation of phosphatidylinositol-3-kinase and Akt after insulin binding to its cell surface receptors is essential for insulin-stimulated GLUT4 translocation [7,8]. AS160, a substrate of Akt, which mediates insulin effects on the machinery of GLUT4 storage vesicle (GSV) translocation, possesses a GAP domain and regulates the activity of Rab protein(s) involved in GLUT4 trafficking [9,10]. When phosphorylated by Akt, as in the case of insulin stimulation, the GAP domain of AS160 loses its activity against Rab-GTP and allows Rab(s) to shift from the GDP- to GTP-binding form [10–12]. Rab in the GTP-binding form recruits various downstream effectors to facilitate transport of GSVs from intracellular localizations to the cell periphery [13–15].

Intracellular cargo transport could occur through microtubules and it has been observed that GSVs moved along microtubules by a variety of experiments [16–18]. However, the physiological significance of this

Abbreviations
EGFP, enhanced green fluorescence protein; GLUT4, glucose transporter 4; GSV, GLUT4 storage vesicle; PC, percentage colocalization; PM, plasma membrane; TIRFM, total internal reflection fluorescence microscopy.

transport in insulin-stimulated GLUT4 translocation remains controversial. The idea that transport of GSVs along microtubules is indispensable for insulin-stimulated GLUT4 translocation is supported by studies demonstrating that microtubule-depolymerizing agents inhibit insulin-stimulated glucose uptake and GLUT4 translocation [19–21] and perturbation of the function of kinesin retards insulin-stimulated GLUT4 translocation [16,18]. However, other data show that microtubule disruption had no effect on GLUT4 translocation and that some reagents involved in the experiments mentioned above attenuated glucose uptake by microtubule-independent manner [22,23]. More recently, Eyster *et al.* [24] noted that microtubules were involved in more than simply transport of GSVs [24].

Thus, as one important route for intracellular cargo transport, the exact role played by microtubules in insulin-stimulated GLUT4 translocation remains elusive. In the present study, we used total internal reflection fluorescence microscopy (TIRFM) to investigate the functions of microtubules in the trafficking of enhanced green fluorescence protein (EGFP)-tagged GLUT4 in 3T3-L1 adipocytes. Our results suggest that intact microtubules are obligatory for insulin-stimulated GLUT4 translocation.

Results

Insulin-stimulated GLUT4 translocation to the PM requires intact microtubules

In all experiments, 3T3-L1 adipocytes were electroporated with GLUT4-EGFP plasmid [25] to label GSVs *in vivo*. For disruption of microtubules, 3T3-L1 adipocytes were pretreated with 33 μM nocodazole for 1 h and the same concentration of nocodazole was present in external buffer throughout experiments to prevent microtubules from repolymerization. This treatment has been confirmed to completely depolymerize microtubules and has been widely employed [16,19,24]. Control and nocodazole-pretreated adipocytes were incubated with 100 nM insulin and observed under TIRFM for 30 min to monitor the insulin-stimulated GLUT4-EGFP translocation to the PM. Insulin caused GLUT4 to move from intracellular pools to the PM in control adipocytes, resulting in a net gain of GLUT4 on the PM, as reflected by the consecutive augmentation of fluorescence intensity of GLUT4-EGFP in the cell footprint and gradual blurring of the punctas projected by GSVs underneath the PM (Fig. 1A, upper row). In nocodazole-pretreated adipocytes, the increase of fluorescence intensity was diminished substantially, and single GSVs underneath the PM still could be distinguished until 21 min after insulin perfusion (Fig. 1A, lower row). These results

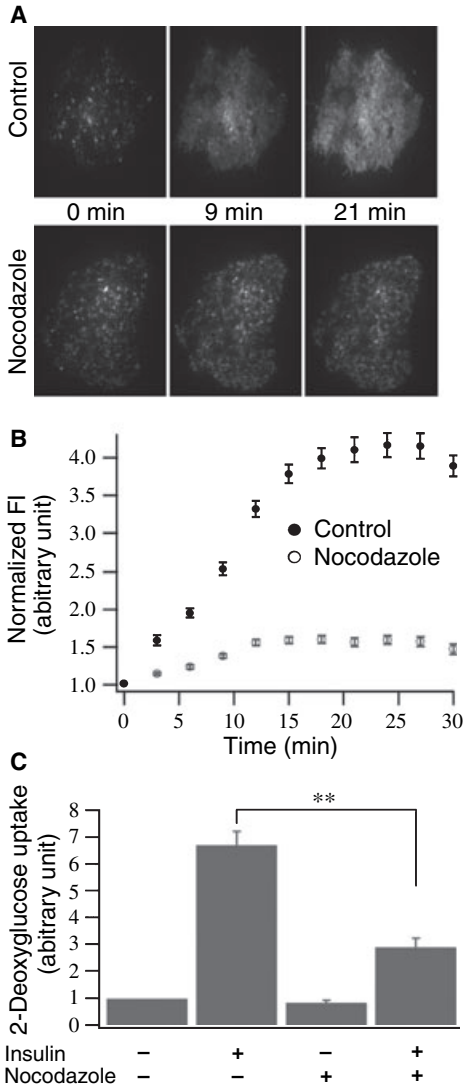

Fig. 1. Microtubule disruption inhibited insulin-stimulated GLUT4 translocation to the PM and attenuated glucose uptake. (A) Microtubule disruption diminished GLUT4 translocation to the PM. Adipocytes, electroporated with GLUT4-EGFP plasmid, were treated with or without nocodazole, and then observed under TIRFM for 30 min to monitor the insulin-stimulated GLUT4-EGFP translocation to the PM. Images captured at different time points are shown; 100 nM insulin was perfused at 0 min. (B) Quantification of the time course of GLUT4 translocation to the PM. Fluorescence intensity of images were normalized by intensity of the image acquired before insulin perfusion (0 min). Control, $n = 5$ cells; nocodazole, $n = 6$ cells. Data are the mean ± SEM. (C) Insulin-stimulated glucose uptake was attenuated by microtubule disruption. Glucose uptake was measured at indicated conditions and readouts were normalized by the mean value of basal condition in the same batch. Error bars indicate the SEM from three independent experiments. $^{**}P < 0.01$.

reveal that less GLUT4 was translocated to the PM in nocodazole-treated adipocytes. Quantification of GLUT4 translocation (Fig. 1B) reveals that insulin stimulation resulted in an approximate four-fold increase of fluorescence intensity in the cell footprint in control adipocytes. Nocodazole treatment shrunk the maximum fluorescence intensity to approximately 1.5-fold over basal intensity. The reduction of intensity change indicates that microtubule disruption inhibited GLUT4 translocation to the PM by approximately 80%. To confirm the inhibitory effect of microtubule disruption on GLUT4 translocation observed by TIRFM, glucose uptake measurement was executed. Insulin stimulation increased glucose uptake by approximately six-fold in control adipocytes, and microtubule disruption reduced this increase by approximately 50% (Fig. 1C). Taken together, these data suggest that microtubule disruption inhibits GLUT4 translocation to the PM and a lack of GLUT4 on the PM slows down glucose transport.

Disruption of microtubules restricts long-range lateral movement of GSVs

It was observed that some GSVs underwent long-range lateral movement in the TIRF zone. These movements appeared to be directional and took place along some predefined tracks (supplementary Video S1). After treatment with nocodazole, this type of movement diminished. To depict this finding, in each cell, the longest three tracks of lateral movement of GSVs were identified. The representative result shows that, in control cells, all of the identified tracks stretched for several micrometers. Nevertheless, in nocodazole-treated cells, all tracks were shorter than 2 μm (Fig. 2A). The statistical data (Fig. 2B) demonstrate that, in control adipocytes, the identified tracks were generally in the range 4–9 μm and microtubule disruption shifted this distribution to the shorter range. Disappearance of directional long-range lateral movement of GSVs after nocodazole treatment suggests that this type of movement is along the microtubule.

Mobility of GSVs is attenuated by microtubule disruption

In the TIRF zone, the movement of GSVs is dynamic. Usually, they enter into TIRF zone and stay immobilized at one position for a period, which is termed 'docking' [17,26,27]. Then they either fuse with the PM or return back to the cytosol (supplementary Video S2). The typical docking time has been determined to be approximately 6 s [26,27]. This means

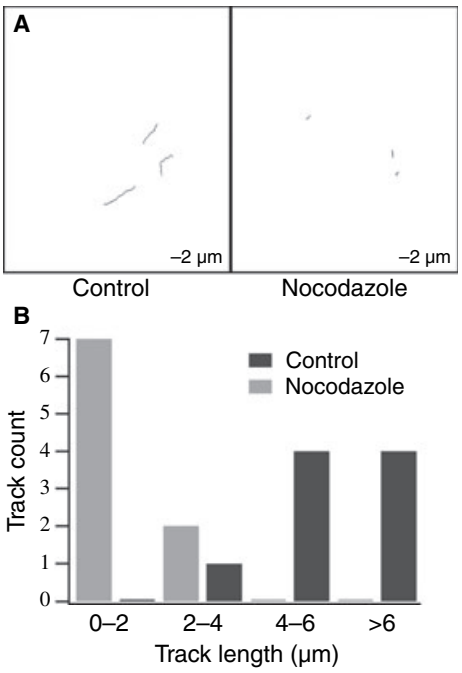

Fig. 2. Intracellular long-range lateral movement of GSV was dependent on intact microtubules. (A) The longest three tracks were identified from single control and nocodazole-treated adipocytes, respectively. GSVs were tracked in the absence of insulin stimulation. (B) Histogram of the length of the longest three lateral transport tracks. For each cell, only the longest three tracks are included into the statistics (n = 3 cells for both conditions).

that GSVs are transported to and away from the cell periphery constitutively in 3T3-L1 adipocytes and, in this manner, GSVs interact with the PM in turn. Intriguingly, a population of GSVs lost their mobility in microtubule-disrupted adipocytes. These GSVs stayed at the same position for a long time (> 100 s), without any detectable movement (supplementary Video S3). This kind of immobilized state is different from the docking state because GSVs hardly dock at the PM for longer than 50 s [26,27]. We depicted the loss of mobility of GSVs using the method described by Huang *et al.* [27]. First, a pair of images acquired at a certain time interval was taken. GSVs in the preceding image were stained green, and those in the subsequent one were stained red. Then the two images were merged. When the time interval was short (Δt = 1 s), there were numerous GSVs stained with yellow in both conditions (Fig. 3A, upper row). In control conditions, docking GSVs could stay at the same position for approximately 6 s, accounting for most of these yellow vesicles. In the case of microtubule disruption, both docking and loss-of-mobility GSVs could contribute to these yellow ones. When the

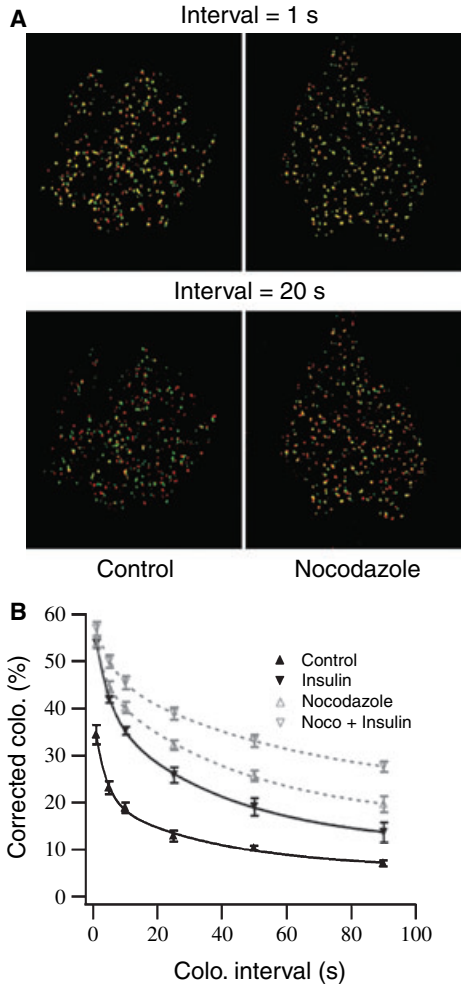

Fig. 3. Microtubule disruption reduced the mobility of GSVs. (A) Microtubule disruption caused a population of GSVs to lose their mobility. Image pairs, captured at the time interval of 1 s and 20 s, were stained with different colors. Green was assigned to GSVs in the proceeding image and red to those in the subsequent one. These two images were then overlayed. Yellow images represent vesicles which stay at the same position during the time interval. All image pairs were acquired in the absence of insulin stimulation. (B) Corrected PC values at intervals of 1, 5, 10, 25, 50 and 90 s were calculated. Lines represent fits of these data by two-exponential decay function. Control, $n = 5$ cells; nocodazole, $n = 7$ cells.

time interval was prolonged to 20 s ($\Delta t = 20$ s), and because the time interval was much longer (by more than three-fold) than the average docking time, docking GSVs could no longer appear at the same position in both images. Thus, there was little overlap between vesicles at this interval in control conditions. Microtubule disruption increased the degree of overlap, indicated by the denser yellow vesicles (Fig. 3A, lower row). This result demonstrates that microtubule disruption immobilized a group of GSVs at the same position for longer than 20 s. For quantification, corrected percentage colocalization (PC) values were calculated. The PC value describes how the degree of overlap between a pair of images changes along with time interval prolongation [27]. As reported previously, insulin stimulation reduced the mobility of GSVs, indicated by the elevated PC value (Fig. 3B). When microtubules were disrupted, the mobility of GSVs decreased further and the corresponding PC values were elevated over that from insulin-stimulated adipocytes. When comparing the PC values measured from insulin-stimulated control and nocodazole-treated adipocytes, it is obvious that PC values from the two conditions were almost equal to each other at short intervals (1 and 5 s) and that the difference became more obvious at longer intervals. For microtubule-disrupted cells, because the loss-of-mobility GSVs stayed immobilized for a longer time, PC values were more resistant to time interval prolongation. It is likely that the lack of transport tracks resulting from microtubule disruption leaves GSVs unable to move, either laterally or perpendicularly.

Microtubule disruption inhibits the recruitment of GSVs to underneath the PM

To determine whether microtubules play a role(s) in transport of GSVs to the cell periphery, we aimed to quantify this transport. Since GSVs are approaching and leaving the PM constitutively, the density of GSVs underneath the PM directly reflects the capability of this transport. Because the loss-of-mobility GSVs are excluded from this transport, they should not be included in this density. We subtracted them from the density by defining a loss-of-mobility GSV as one staying immobilized underneath the PM for longer than 50 s. This definition excluded most docking GSVs from subtraction and identified the loss-of-mobility GSVs precisely. As shown in Fig. 4A, insulin stimulation slightly increased the density of GSVs adjacent to the PM. Nocodazole treatment reduced GSVs underneath the PM and deprived insulin of its ability to increase this density. This finding indicates that the transport of GSVs to the cell periphery is microtubule-dependent. Docking analysis [26,27] reveals that insulin increased docking rate by approximately two-fold and microtubule disruption almost abolished the docking of GSVs at the PM (Fig. 4B). These results suggest that functional GSVs, which docked at the PM in control cells, were essentially absent from the cell periphery of microtubule-disrupted adipocytes, although the vesicle density remained approximately 50% of that in

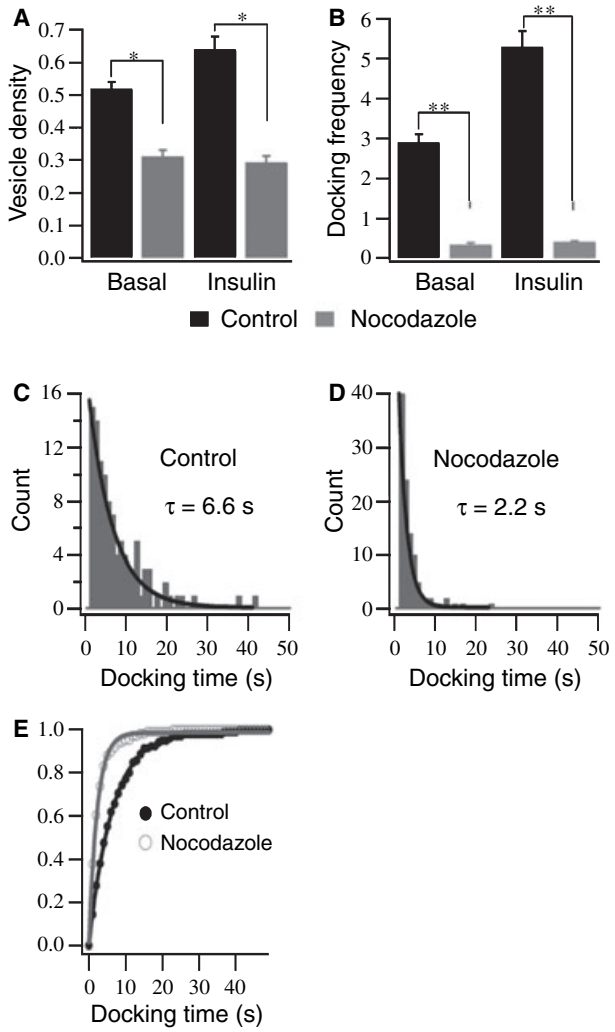

Fig. 4. Microtubule disruption inhibited the recruitment of GSVs to underneath the PM. (A) Nocodazole reduced the density (in vesicle·μm^{-2}) of GSVs underneath the PM. Control, $n = 4$ cells; nocodazole, $n = 7$ cells (*$P < 0.05$). (B) Nocodazole treatment almost abolished the docking of GSVs at the PM (in 10^{-3} event·μm^{-2}·s^{-1}). Control, $n = 3$ cells; nocodazole, $n = 5$ cells (**$P < 0.01$). (C) Docking time distribution of 90 docking events from control adipocytes. (D) Docking time distribution of 66 docking events from nocodazole-treated adipocytes. (E) Docking events from control and microtubule-disrupted adipocytes exhibited different characteristics. The time constant of docking process (τ) was approximately 6 s and 2 s, respectively (**$P < 0.01$; Kolmogorov–Smirnov and Mann–Whitney tests).

control cells. The duration of docking state was determined by analyzing their stochastic behavior. Docking time distributions from control and microtubule-disrupted adipocytes are shown in Fig. 4C,D. It is evident that the remaining docking events in microtubule-disrupted adipocytes exhibited transient time processes, and these obviously are different from those in control cells. The cumulative distribution of docking time makes this difference easier to observe (Fig. 4E). The time constant of the docking process (τ) was approximately 2 s in microtubule-disrupted adipocytes, and approximately 6 s in control cells. Thus, disruption of microtubules blocked functional docking of GSVs at the PM.

Discussion

In the present study, the physiological significance of intact microtubules in insulin-stimulated GLUT4 translocation was investigated in 3T3-L1 adipocytes by TIRFM. First, it was observed that nocodazole treatment reduced GLUT4 translocation to the PM, which was demonstrated by a decreased fluorescence intensity change in the cell footprint and less blurring of punctas projected by GSVs underneath the PM. In previous studies, which provided negative data concerning this function of nocodazole, either a lower concentration of nocodazole was used [22,23], which was shown to be incapable of fully disrupting microtubules [19], or a different quantification method was involved [22], which may differ from our system with respect to sensitivity. Thus, from our data, we propose that intact microtubules are essential for insulin-stimulated GLUT4 translocation to the PM. Of note, there remains a small population of GLUT4 translocated to the PM in microtubule-disrupted adipocytes. This is in agreement with the findings obtained in primary adipocytes [28] and suggests that there are two different pools of GLUT4 with different microtubule dependency in 3T3-L1 adipocytes.

Second, the long-range lateral movements of GSVs were investigated under TIRFM. These movements followed some predefined tracks, presumably the microtubule networks [17,29], and vanished after nocodazole treatment. This finding is consistent with previous observations made under confocal microscopy, which visualized long-range transport of GSVs along the microtubule and also demonstrated that disruption of microtubules and perturbation of the function of kinesin blocked this type of movement [18,21]. Therefore, our data provide further support for the hypothesis that GSVs undergo microtubule-based long-range directional movement in 3T3-L1 adipocytes.

Third, although it was reported by another group that nocodazole treatment did not reduce GSVs underneath the PM [29], the finding of loss-of-mobility GSVs in microtubule-disrupted adipocytes enabled us to quantify the transport capacity of the microtubule system more precisely. With this improved calculation,

it was found that there were less GSVs underneath the PM in nocodazole-treated adipocytes. The lack of GSVs transported to the cell periphery indicates that microtubules support the transport of GSVs to the cell periphery. This finding may have critical significance with respect to the physiological identity of GSVs. GLUT1 and transferring receptor, which are resident proteins in recycling endosome, can be translocated to the PM independent of microtubules [21,30,31]. Thus, our data support the idea that GSVs are specific organelles that do not overlap with the recycling endosome and need microtubules when approaching the PM.

Fourth, the observation that docking of GSVs at the PM was almost abolished by microtubule disruption demonstrates that there are no functional GSVs left underneath the PM in microtubule-disrupted adipocytes, further indicating that transport of functional GSVs to the cell periphery requires intact microtubules. Further stochastic behavior analysis revealed that the remaining docking events in microtubule-disrupted adipocytes are different in nature from those in control cells. Thus, the transient docking GSVs in the absence of microtubules are different from the majority of docking GSVs in control cells. The docking GSVs remaining after microtubule disruption presumably come from the microtubule-independent pool of GLUT4, although the possibility that microtubules directly regulated the docking process of GSVs cannot be fully ruled out [24]. In summary, our data reveal that transport of GSVs along microtubules to underneath the PM is required in insulin-stimulated GLUT4 translocation.

Experimental procedures

Cell culture and transfection

The 3T3-L1 cells were cultured in high-glucose DMEM (Gibco BRL, Grand Island, NY, USA) supplemented with 10% foetal bovine serum (Gibco) at 37 °C and 5% CO_2. Two days after confluence, the cells were switched into differentiation medium containing 10% fetal bovine serum (Gibco), 1 μM bovine insulin, 0.5 mM 3-isobutyl-1-methylxanthine and 0.25 μM dexamethasone. Two days later, the medium was changed with 10% fetal bovine serum and 1 μM bovine insulin for another 2 days. The cells were then maintained in DMEM with 10% fetal bovine serum. Seven days after differentiation, 3T3-L1 adipocytes were treated with 0.05% trypsin-EDTA (Gibco) and washed twice with Opti-MEM (Gibco) by centrifugation at 1000 ***g*** at room temperature. The cells were resuspended in Opti-MEM (Gibco), and 40 mg GLUT4-EGFP plasmid was added to a final volume of 800 mL. Cells were then electroporated at 360 V for 10 ms using a BTX 830 electroporator (Genetronics Inc., San Diego, CA, USA) and plated on coverslips coated with poly-L-lysine. Experiments were performed 2 days after transfection in KRBB solution containing 129 mM NaCl, 4.7 mM KCl, 1.2 mM KH_2PO_4, 5 mM $NaHCO_3$, 10 mM HEPES, 3 mM glucose, 2.5 mM $CaCl_2$, 1.2 mM $MgCl_2$ and 0.1% BSA (pH 7.2). Prior to the experiments, adipocytes were serum starved for 2 h and transferred to a home-made closed perfusion chamber. All experiments were performed at 30 °C. Insulin was applied at a final concentration of 100 nM throughout the study. Unless otherwise stated, all drugs were purchased from Sigma (St Louis, MO, USA).

2-Deoxyglucose uptake

The 3T3-L1 adipocytes were serum starved for 2 h at 37 °C and treated with or without nocodazole for 1 h. Then cell were washed three times with KRPH buffer [5 mM Na_2HPO_4, 20 mM Hepes (pH 7.4), 1 mM $MgSO_4$, 1 mM $CaCl_2$, 136 mM NaCl, 4.7 mM KCl, and 1% BSA]. Glucose transport was determined at 37 °C by incubation with 50 mM 2-deoxyglucose uptake containing 0.5 mCi of 2-[^{3}H] deoxyglucose. The reaction was stopped after 5 min by washing the cells three times with ice-cold NaCl/Pi. The cells were solubilized in 1% Triton X-100 at 37 °C for 30 min, and aliquots were subjected to scintillation counting. All readouts were normalized by the mean value measured from the control condition in the same batch, and three independent experiments were conducted.

TIRFM imaging

The TIRFM setup was constructed based on through-the-lens configuration as described previously [25]. The penetration depth of the evanescent field was estimated to be 113 nm by measuring the incidence angle with a prism (n = 1.518) 488-nm laser beam.

Data analysis

For quantification of the time course of GLUT4 translocation, acquired images were processed. First, the cell boundary was detected by a bespoke program developed in Matlab (The Math Works Inc., Natick, MA, USA) [26]. Next, mean fluorescence intensity in cell boundary was measured. Finally, mean values from different time points were normalized by the value from 0 min. The ImageJ plugin 'Manual tracking' (NIH Image, Bethesda MD, USA) was utilized to track GSVs. In each cell, lateral movements of GSVs were identified and the longest three movements were selected out for further analysis. For description of the mobility, GSVs were automatically segmented from the background by an intensity-based threshold [26]. For

calculation of corrected PC values, image stacks acquired at 5 Hz were used. First, GSVs in each image were identified. Next, all images in stacks were converted into binary images, in which GSVs comprised the foreground and other pixels comprised the background. Then, corrected PC values were calculated according to the method described by Huang *et al.* [27]. A docking event is defined as previously described [26], and analysis was constrained to those GSVs, that went through whole docking process (coming into the TIRF zone–immobilized–retrieving or fusion) during image acquisition. The loss-of-mobility GSVs, which stayed immobilized throughout image acquisition, were precluded from the vesicle docking assay. The mean docking time was determined by exponential fitting to its distribution.

Statistical analysis

For normally distributed data, population averages are given as mean ± SEM and statistical significance was tested using Student's *t*-test. Statistical significance between exponential distributions was assessed using Kolmogorov–Smirnov and Mann–Whitney tests.

Acknowledgements

This work was supported by grants from the National Science Foundation of China (30670504 and 30630020), the Major State Basic Research Program of China (2004CB720000) and the CAS Project (KSCX1-YW-02-1). The laboratory of T.X. belongs to a Partner Group Scheme of the Max Planck Institute for Biophysical Chemistry (Göttingen, Germany). We thank Dr Terrence Tiersch from Louisiana State University for critically reading the manuscript. We also thank Dr Jing Zhao for technical assistance.

References

1 Huang S & Czech MP (2007) The GLUT4 glucose transporter. *Cell Metab* **5**, 237–252.
2 Watson RT, Kanzaki M & Pessin JE (2004) Regulated membrane trafficking of the insulin-responsive glucose transporter 4 in adipocytes. *Endocr Rev* **25**, 177–204.
3 Bryant NJ, Govers R & James DE (2002) Regulated transport of the glucose transporter GLUT4. *Nat Rev* **3**, 267–277.
4 Karylowski O, Zeigerer A, Cohen A & McGraw TE (2004) GLUT4 is retained by an intracellular cycle of vesicle formation and fusion with endosomes. *Mol Biol Cell* **15**, 870–882.
5 Holman GD, Lo Leggio L & Cushman SW (1994) Insulin-stimulated GLUT4 glucose transporter recycling. A problem in membrane protein subcellular trafficking through multiple pools. *J Biol Chem* **269**, 17516–17524.
6 Satoh S, Nishimura H, Clark AE, Kozka IJ, Vannucci SJ, Simpson IA, Quon MJ, Cushman SW & Holman GD (1993) Use of bismannose photolabel to elucidate insulin-regulated GLUT4 subcellular trafficking kinetics in rat adipose cells. Evidence that exocytosis is a critical site of hormone action. *J Biol Chem* **268**, 17820–17829.
7 Martin SS, Haruta T, Morris AJ, Klippel A, Williams LT & Olefsky JM (1996) Activated phosphatidylinositol 3-kinase is sufficient to mediate actin rearrangement and GLUT4 translocation in 3T3-L1 adipocytes. *J Biol Chem* **271**, 17605–17608.
8 Okada T, Kawano Y, Sakakibara T, Hazeki O & Ui M (1994) Essential role of phosphatidylinositol 3-kinase in insulin-induced glucose transport and antilipolysis in rat adipocytes. Studies with a selective inhibitor wortmannin. *J Biol Chem* **269**, 3568–3573.
9 Kane S, Sano H, Liu SC, Asara JM, Lane WS, Garner CC & Lienhard GE (2002) A method to identify serine kinase substrates. Akt phosphorylates a novel adipocyte protein with a Rab GTPase-activating protein (GAP) domain. *J Biol Chem* **277**, 22115–22118.
10 Miinea CP, Sano H, Kane S, Sano E, Fukuda M, Peranen J, Lane WS & Lienhard GE (2005) AS160, the Akt substrate regulating GLUT4 translocation, has a functional Rab GTPase-activating protein domain. *Biochem J* **391**, 87–93.
11 Larance M, Ramm G, Stockli J, van Dam EM, Winata S, Wasinger V, Simpson F, Graham M, Junutula JR, Guilhaus M *et al.* (2005) Characterization of the role of the Rab GTPase-activating protein AS160 in insulin-regulated GLUT4 trafficking. *J Biol Chem* **280**, 37803–37813.
12 Eguez L, Lee A, Chavez JA, Miinea CP, Kane S, Lienhard GE & McGraw TE (2005) Full intracellular retention of GLUT4 requires AS160 Rab GTPase activating protein. *Cell Metab* **2**, 263–272.
13 Grosshans BL, Ortiz D & Novick P (2006) Rabs and their effectors: achieving specificity in membrane traffic. *Proc Natl Acad Sci USA* **103**, 11821–11827.
14 Spang A (2004) Vesicle transport: a close collaboration of Rabs and effectors. *Curr Biol* **14**, R33–R34.
15 Sano H, Eguez L, Teruel MN, Fukuda M, Chuang TD, Chavez JA, Lienhard GE & McGraw TE (2007) Rab10, a target of the AS160 Rab GAP, is required for insulin-stimulated translocation of GLUT4 to the adipocyte plasma membrane. *Cell Metab* **5**, 293–303.
16 Emoto M, Langille SE & Czech MP (2001) A role for kinesin in insulin-stimulated GLUT4 glucose transporter translocation in 3T3-L1 adipocytes. *J Biol Chem* **276**, 10677–10682.

17 Lizunov VA, Matsumoto H, Zimmerberg J, Cushman SW & Frolov VA (2005) Insulin stimulates the halting, tethering, and fusion of mobile GLUT4 vesicles in rat adipose cells. *J Cell Biol* **169**, 481–489.
18 Semiz S, Park JG, Nicoloro SM, Furcinitti P, Zhang C, Chawla A, Leszyk J & Czech MP (2003) Conventional kinesin KIF5B mediates insulin-stimulated GLUT4 movements on microtubules. *EMBO J* **22**, 2387–2399.
19 Olson AL, Eyster CA, Duggins QS & Knight JB (2003) Insulin promotes formation of polymerized microtubules by a phosphatidylinositol 3-kinase-independent, actin-dependent pathway in 3T3-L1 adipocytes. *Endocrinology* **144**, 5030–5039.
20 Olson AL, Trumbly AR & Gibson GV (2001) Insulin-mediated GLUT4 translocation is dependent on the microtubule network. *J Biol Chem* **276**, 10706–10714.
21 Fletcher LM, Welsh GI, Oatey PB & Tavare JM (2000) Role for the microtubule cytoskeleton in GLUT4 vesicle trafficking and in the regulation of insulin-stimulated glucose uptake. *Biochem J* **352** Pt 2, 267–276.
22 Molero JC, Whitehead JP, Meerloo T & James DE (2001) Nocodazole inhibits insulin-stimulated glucose transport in 3T3-L1 adipocytes via a microtubule-independent mechanism. *J Biol Chem* **276**, 43829–43835.
23 Shigematsu S, Khan AH, Kanzaki M & Pessin JE (2002) Intracellular insulin-responsive glucose transporter (GLUT4) distribution but not insulin-stimulated GLUT4 exocytosis and recycling are microtubule dependent. *Mol Endocrinol (Baltimore, MD)* **16**, 1060–1068.
24 Eyster CA, Duggins QS, Gorbsky GJ & Olson AL (2006) Microtubule network is required for insulin signaling through activation of Akt/protein kinase B: evidence that insulin stimulates vesicle docking/fusion but not intracellular mobility. *J Biol Chem* **281**, 39719–39727.
25 Li CH, Bai L, Li DD, Xia S & Xu T (2004) Dynamic tracking and mobility analysis of single GLUT4 storage vesicle in live 3T3-L1 cells. *Cell Res* **14**, 480–486.
26 Bai L, Wang Y, Fan J, Chen Y, Ji W, Qu A, Xu P, James DE & Xu T (2007) Dissecting multiple steps of GLUT4 trafficking and identifying the sites of insulin action. *Cell Metab* **5**, 47–57.
27 Huang S, Lifshitz LM, Jones C, Bellve KD, Standley C, Fonseca S, Corvera S, Fogarty KE & Czech MP (2007) Insulin stimulates membrane fusion and GLUT4 accumulation in clathrin coats on adipocyte plasma membranes. *Mol Cell Biol* **27**, 3456–3469.
28 Liu LB, Omata W, Kojima I & Shibata H (2003) Insulin recruits GLUT4 from distinct compartments via distinct traffic pathways with differential microtubule dependence in rat adipocytes. *J Biol Chem* **278**, 30157–30169.
29 Xu YK, Xu KD, Li JY, Feng LQ, Lang D & Zheng XX (2007) Bi-directional transport of GLUT4 vesicles near the plasma membrane of primary rat adipocytes. *Biochem Biophys Res Commun* **359**, 121–128.
30 Sakai T, Yamashina S & Ohnishi S (1991) Microtubule-disrupting drugs blocked delivery of endocytosed transferrin to the cytocenter, but did not affect return of transferrin to plasma membrane. *J Biochem* **109**, 528–533.
31 Ducluzeau PH, Fletcher LM, Vidal H, Laville M & Tavare JM (2002) Molecular mechanisms of insulin-stimulated glucose uptake in adipocytes. *Diabetes Metab* **28**, 85–92.

Supplementary material

The following supplementary material is available online:

Video S1. One GSV moved laterally in the TIRF zone. The rectangle indicates the docking process. Scale bar = 1 μm.

Video S2. GSVs were approaching and leaving the PM constitutively. Rectangles indicate the docking-retrieving events and circles indicate the docking-fusion events.

Video S3. A group of GSVs stayed immobilized underneath the PM throughout image acquisition, which lasted for 100 s.

This material is available as part of the online article from http://www.blackwell-synergy.com

Please note: Blackwell Publishing are not responsible for the content or functionality of any supplementary materials supplied by the authors. Any queries (other than missing material) should be directed to the corresponding author for the article.